Progress In Electromagnetics Research Letters, Vol. 95, 43–53, 2021

SRR Loaded Compact Tri-Band MIMO Antenna for WLAN/WiMAX Applications

Venkatesan Rajeshkumar[1] and Rengasamy Rajkumar[2, *]

Abstract—A multiband four-element multiple-input-multiple-output (MIMO) antenna configuration is proposed. The antenna consists of split ring resonators (SRRs) along with an inverted L-shaped monopole antenna (ILA) structure on the top of the substrate and a slotted ground plane. The antenna without the SRRs exhibits resonances at 2.4 GHz, 3.66 GHz, and 5.5 GHz with the impedance bandwidth (IBW) of 14.5%, 35.1%, and 9.6%, respectively. With the addition of SRRs, the antenna exhibits additional resonance at 5.1 GHz with improved bandwidth and minimizes the reflections. Consequently, the impedance bandwidth at 5 GHz frequency band gets improved to 17.2%. Overall, the proposed antenna will cover the 2.4 GHz wireless local area network (WLAN) & industrial, scientific, medical (ISM) band, 3.5 GHz worldwide interoperability for microwave access (WiMAX), and 5 GHz WLAN 4G/5G applications. In spite of very compact area ($0.094\lambda_0^2$, for the highest operating wavelength) and presence of common ground, the antenna exhibits high inter-element isolation of ≥ -14 dB and $S_{11} \geq -10$ dB. The proposed antenna design is fabricated, tested, and analyzed.

1. INTRODUCTION

Multi-input and multi-output (MIMO) technology has excited the world of research because of its conceivable applications in digital-televisions, metropolitan area networks, wireless local area networks (WLAN), and mobile communications like the fourth generation (4G), long term evolution (LTE), and 5G wireless communications, for its capacity of upgrading effectiveness inside limited power levels and bandwidth [1–3]. The main challenge in designing a MIMO antenna within a small space is to reduce the mutual coupling between different elements of the antenna by this process, and the severe damage can be avoided which is caused by coupling. The coupling has to be avoided by increasing the inter-element isolation, but acquiring high isolation within the small size is a complex problem in the research of MIMO antenna systems. Various cases and methods to overcome these problems along with improving isolation and envelope correlation coefficient are discussed in [4, 5]. A solution to achieve maximum channel capacity with multiport matching is proposed in [6]. In [7–9], researchers employed a ground slot to increase isolation.

In order to support the utilization of MIMO orthogonal data streams for increasing the channel capacity of various microwave applications like Wi-Fi, WiMAX, WLAN are proposed in [10–25]. Conventional microstrip patch antenna can be used to realize MIMO response by using various isolation techniques which are discussed in [10–13]. A three-folds fork-shaped stub is introduced in the ground plane to improve the isolation [10]. In [11], a DGS structure is introduced in the ground plane of the antenna to enhance the gain value which is obtained due to parasitic capacitance. A mushroom based EBG and a fractal-based structure are used between the two antenna designs to improve the

Received 7 October 2020, Accepted 5 December 2020, Scheduled 14 December 2020
* Corresponding author: Rengasamy Rajkumar (imesanai@gmail.com).
[1] Department of Communication Engineering, School of Electronics Engineering (SENSE), VIT Vellore, Tamilnadu, India.
[2] Department of Electronics and Communication Engineering, Vel Tech Rangarajan Dr Sagunthala R&D Institute of Science and Technology, Avadi, Chennai, India.

isolation [12]. Metamaterial based CSRR semicircles are introduced in the ground plane for the reduction of mutual coupling [13]. The above antenna designs [10–13] have better isolation in the desired frequencies. However, they cover only a single resonance frequency band.

Multiband MIMO antenna performance is realized by using the different shapes of radiating elements, and a modified rectangular stair shaped radiating element with a ring-shaped ground plane is used [14]. A dipole with a V-shaped branch is used to realize the MIMO antenna for impedance matching performance [15]. The recent concentrated area of research is using multiple antenna elements for the implementation of sub-6 GHz (3.4–3.9 GHz) 5G massive MIMO base stations [16, 17]. In [18], two F-shaped monopole antennas are used which produce dual-band response with less isolation, and to enhance the isolation performance a decoupling structure is connected between two antenna structures. Though isolation performance is better, it does require a large size to implement, and bandwidth coverage is low. The antenna design in [19] has L- and E-shaped stubs and a strip respectively along with two rectangle stubs. Further, parasitic elements and DGS are present in the ground plane to improve isolation performance. Two concentric T-shaped monopole antennas are used with a compact size of $43\times38\times1.575\,\text{mm}^3$ to cover the dual-band applications. Though antenna has a compact structure it requires different techniques to improve the isolation level [20]. The design in [21] has an F-shaped monopole antenna structure as a main radiating element, and for improving isolation performance an elliptical shaped slot is introduced in the ground plane. A rectangular parasitic element is added besides an antenna design to enhance the isolation performance. Twenty-first century sees the dawn of using metamaterial inspired resonators for designing very small and compact multi-band antennas [22–25] but for achieving compact wideband performance along with increased inter-element isolation. Four inverted L-monopole antennas along with four SRR structures are introduced to realize dual-band MIMO antenna performance [23]. A partial ground plane with SRR structure [24] is used to realize a wider band MIMO antenna which can be used to cover WLAN/WiMAX/5G applications. In [25], a circularly polarized MIMO antenna is discussed. LC resonators place arms of the printed dipole to realize multiband performance which covers lower frequency applications only.

Many of the above designed antennas have covered single frequency bands [10–13]. The antenna reported in [15] is compact due to the proposed design with wider bandwidth, but it has a low isolation (≈ 10 dB). Further, compared to [17], the use of SRRs in the proposed MIMO antenna improves the isolation (I) by 3 dB with the size reduction of 20% as seen in Table 1. The antenna in [23] has almost all applications as that of the proposed antenna and wide bandwidth. However, it operates in unnecessary frequencies (frequencies having no specific wireless applications) which may cause interference. The design in [24] has good isolation and extremely high bandwidth, but using separate ground planes makes it less suitable for practical applications. Adding to the advantages of the proposed antenna, the antenna supports WLAN band at 5 GHz. Further, many designs cover either lower WLAN or 5G applications, and only a few designs cover both applications. However, higher WLAN frequency is not covered along with other applications in many of the reported designs. In order to address the aforementioned limitations, a four inverted L-shaped monopole antenna with four slots are used, to

Table 1. Comparison of proposed design over other MIMO antenna designs.

Antenna Design Refs.	Total Area (λ_0^2)	Number of resonant bands	Operating Frequency (GHz)	IBW (in %)	I in dB
[14]	0.605	1	1.80	46.8	15
[15]	0.096	1	2.32	60.6	10
[17]	0.131	1	2.70	58.6	11
[22]	0.257	2	1.90	12.4, 14.6	15
[23]	0.103	2	2.4	35.21, 6.86	14
[24]	0.109	1	2.50	96.2	14
This work	0.094	3	2.4	14.5, 37.6, 17.2	14

cover all the applications simultaneously.

In the proposed design, the dimensions of inverted L-shaped monopole antennas (ILA's) are calculated using a quarter wavelength and half wavelength principle. With the addition of SRRs, a new resonance at frequency 5.1 GHz is achieved, and it covers the upper WLAN band. The proposed MIMO antenna resonates at 2.4 GHz, 3.45 GHz, and 5.5 GHz, and the detailed design and validation are discussed in the subsequent sections.

2. PROPOSED ANTENNA CONFIGURATION

Various MIMO antennas were proposed using 2×2, 4×4, and 8×8 orthogonal data streams to increase the channel capacity within the limited space available. The antenna in [23] has been designed using 4×4 orthogonal data streams along with ground that has open slots to produce two operating bands. However, it is less reliable for practical applications as the antenna operates at 2.93 GHz and 5.68 GHz with very large bands covering the unwanted frequencies. The basic structure of the antenna is shown in Fig. 1. It consists of four inverted-L shaped monopoles with microstrip feed and as many SRR elements as radiating elements similar to the antenna proposed in [23] with slotted common ground. By changing the length (l_a) and width (w_m) of the monopole elements the operating frequencies can be changed.

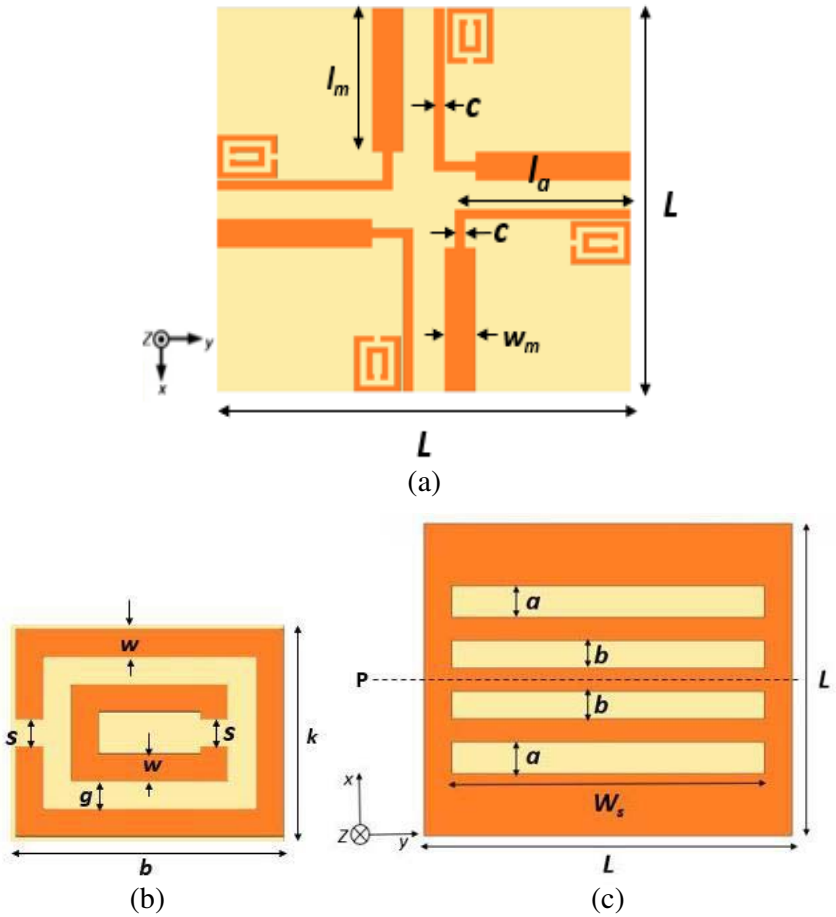

Figure 1. (a) Top view of the proposed antenna, (b) schematic of the SRR unit cell, (c) bottom layer (ground plane) of the antenna.

The dimensions listed in Table 2 have been chosen carefully by considering impedance matching and size restrictions of the system along with the applications for which the antenna is going to be used. The purpose of adding slotted ground in the proposed antenna is to improve the performance of the antenna by increasing the inter-element isolation and to decrease the overall reflection.

Table 2. List of parameters used in the design of the meander line antenna shown in Fig. 1.

List of variables	Value (mm)	List of variables	Value (mm)
W_m	3	b	4.5
c	1	$g = s$	0.6
I_a	17	a	4
l_m	15	b	3.5
L	40	W_s	34
k	5.8	w	0.6

Further, the addition of SRR in the top layer is to enhance the bandwidth of a particular band by designing SRRs resonant frequency closer to the required band. The impact of significant antenna parameters and process of arriving final multiband antenna prototype is explained in the following section along with their simulation and measurement results.

3. RESULTS AND DISCUSSIONS

The proposed antenna design is simulated using Ansoft HFSS. Initially, a 4-inverted L-shaped monopole antenna (4-ILA) with two mid slots is etched in the ground plane of the proposed design, and their responses are illustrated in Fig. 2(a). It is observed that the combined effect of 4-ILA and two slots has produced resonance frequency at 3.5 GHz with a return loss of -12 dB and S_{21} of 11.5 dB. Due to various reasons, the present MIMO antenna systems work for one operating band which is not good for practical use considering the cost of the MIMO antenna system. Therefore, for increasing the number of operating bands, the number of slots in the ground has been increased, which leads to improved return loss (low reflections) and inter-element isolation. The addition and arrangement of the slots are done in a symmetrical way such that the ground always has symmetry from a center line (p) that is drawn along the center of the ground in its equatorial plane as seen in Fig. 1(c).

The dimensions of the slots are chosen in such a way that the radiation from the slots combines with the inverted L-monopole radiation to produce an operating band with the operating frequency at 2.4 GHz. By etching 4 slots in the ground plane, three operating bands (return loss ≥ -10 dB) are obtained, and it is shown in Fig. 2(b). Here a common ground is used in the MIMO system in order to make the design reliable for the practical applications. The first operating band has a center frequency at 2.4 GHz with an impedance bandwidth of 16.66% with return loss (S_{11} in dB) of -27 dB covering the ISM band and the lower bands of WLAN. The other two operating bands have center frequency at 3.66 GHz (IBW of 35.5%) with S_{11} of 17 dB covering the bands of 4G LTE and sub 6 GHz bands used for 5G applications (IBW of 9.6%) with S_{11} of 18.5 dB covering some channels used by higher WLAN band. It is observed that S_{11} and S_{21} performance is improved at 2.4 GHz compared to Fig. 2(a).

Although these results are satisfactory and reliable for practical applications, there is a need to improve the bandwidth at 5.5 GHz which is relatively poor for covering higher WLAN applications. To obtain the desired improvement in the bandwidth, a rectangle-shaped SRR is placed near the 4-inverted L-shaped monopole antenna as shown in Fig. 1(a). The dimensions of the SRR used in the proposed antenna design are shown in Fig. 1(b). The SRR dimensions are chosen to produce a new resonance at 5.1 GHz. The existing antenna response (Fig. 2(b)) has a resonance bandwidth coverage from 5.1 GHz; the newly introduced SRR structure has resonance frequency at 5.1 GHz; 4-ILA and SRR have nearer resonance frequency responses. These two resonances are merged together and produce broader bandwidth (IBW of 17.2) performance at 5.5 GHz as illustrated in Fig. 2(c), improve the bandwidth of the antenna, and cover all the higher WLAN channels effectively.

In the proposed antenna design, the introduced rectangular SRR structure has more impact on the resonance frequency response. SRR is intentionally designed to introduce resonance frequency at 5 GHz, and the proposed SRR response is analyzed using waveguide method as shown Fig. 3(a). The proposed SRR structure is placed over the substrate, and it is filled with air. In the waveguide setup, the top and bottom surfaces are assigned as PMC, and PEC is assigned along the X-axis of the waveguide.

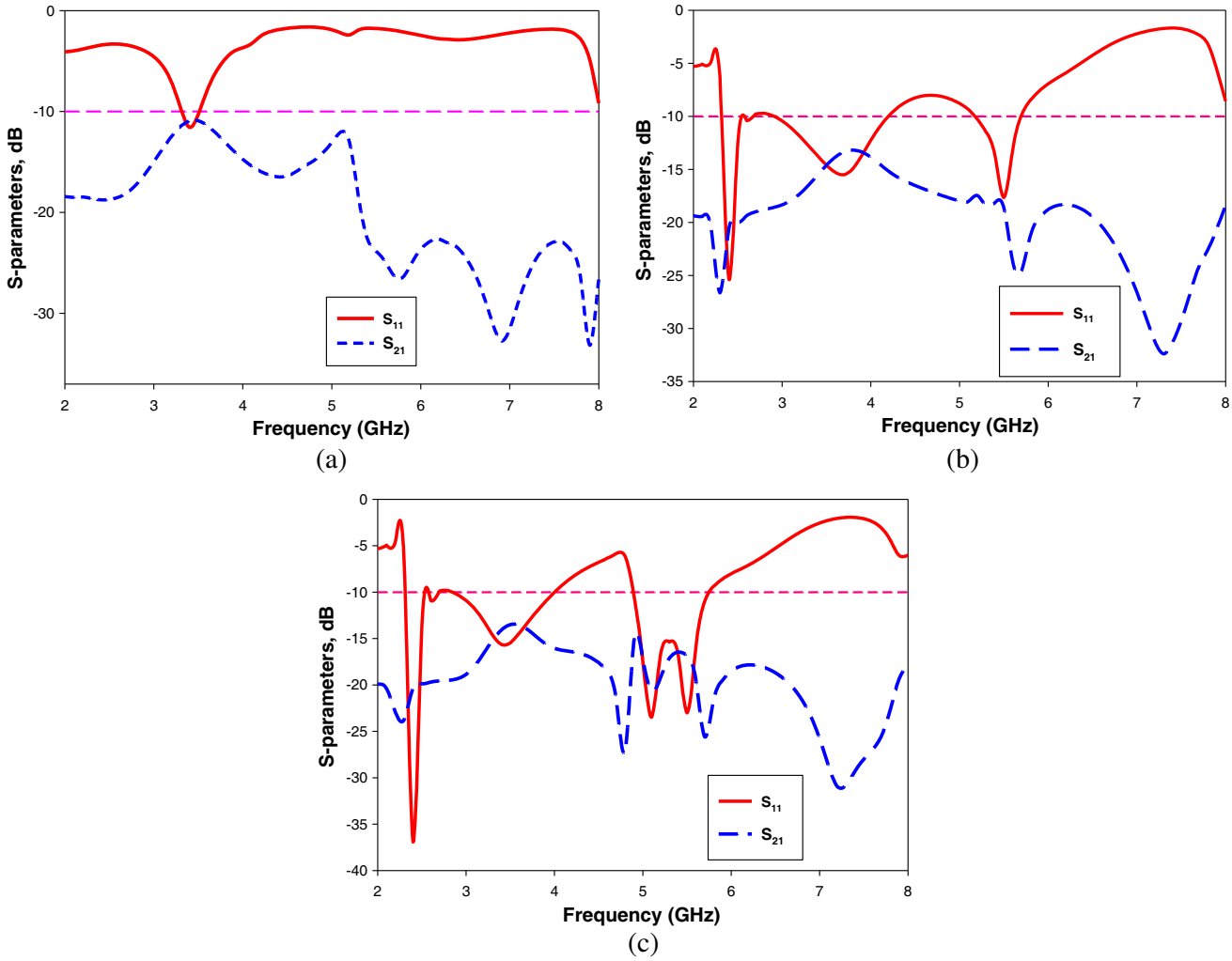

Figure 2. (a) S-parameter graph with the slotted ground with only two slots, (b) S-parameter graph without SRR and (c) S-parameter graph of proposed antenna design.

The other two sides of the waveguide are assigned as port-1 and port-2. By using the above method, S-parameters (S_{11} and S_{21}) of the proposed SRR structure are extracted and illustrated in Fig. 3(b). It is observed that SRR has a resonance response at 5 GHz. From this analysis, it is confirmed that SRR aids in improving the bandwidth performance of the proposed antenna at 5 GHz.

An SRR structure with a given length (k) and breadth (b) of the outer rectangular ring has impact in producing the resonance frequency which can be shifted to lower or higher frequencies based on variations in the parameters of s, w, and g. All the three parameters are varied from 0.4 mm to 0.6 mm, and their responses are plotted in Fig. 3(c). It is observed that fewer variations are observed in the first and second frequency bands for all the parameter variations. At higher frequency (5 GHz), less bandwidth is obtained for 0.4 mm and 0.5 mm while $g = s = w = 0.6$ mm produces better bandwidth response which can be used to cover upper WLAN applications. Similarly, 0.6 mm helps to improve the S_{11} response at a lower frequency (2.4 GHz) compared to other widths and gaps of SRR. From the above analysis, it is concluded that $g = s = w$ of 0.6 mm is fixed as a desired width and gap of the proposed SRR structure.

The design is fabricated, tested, and analyzed; the results such as return loss, isolation, and radiation pattern are in good agreement with the simulation ones.

Figures 4(a) and 4(b) show the comparison of simulated and measured results of return loss and isolation of the proposed antenna. A small discrepancy in the measured results is attributed to soldering

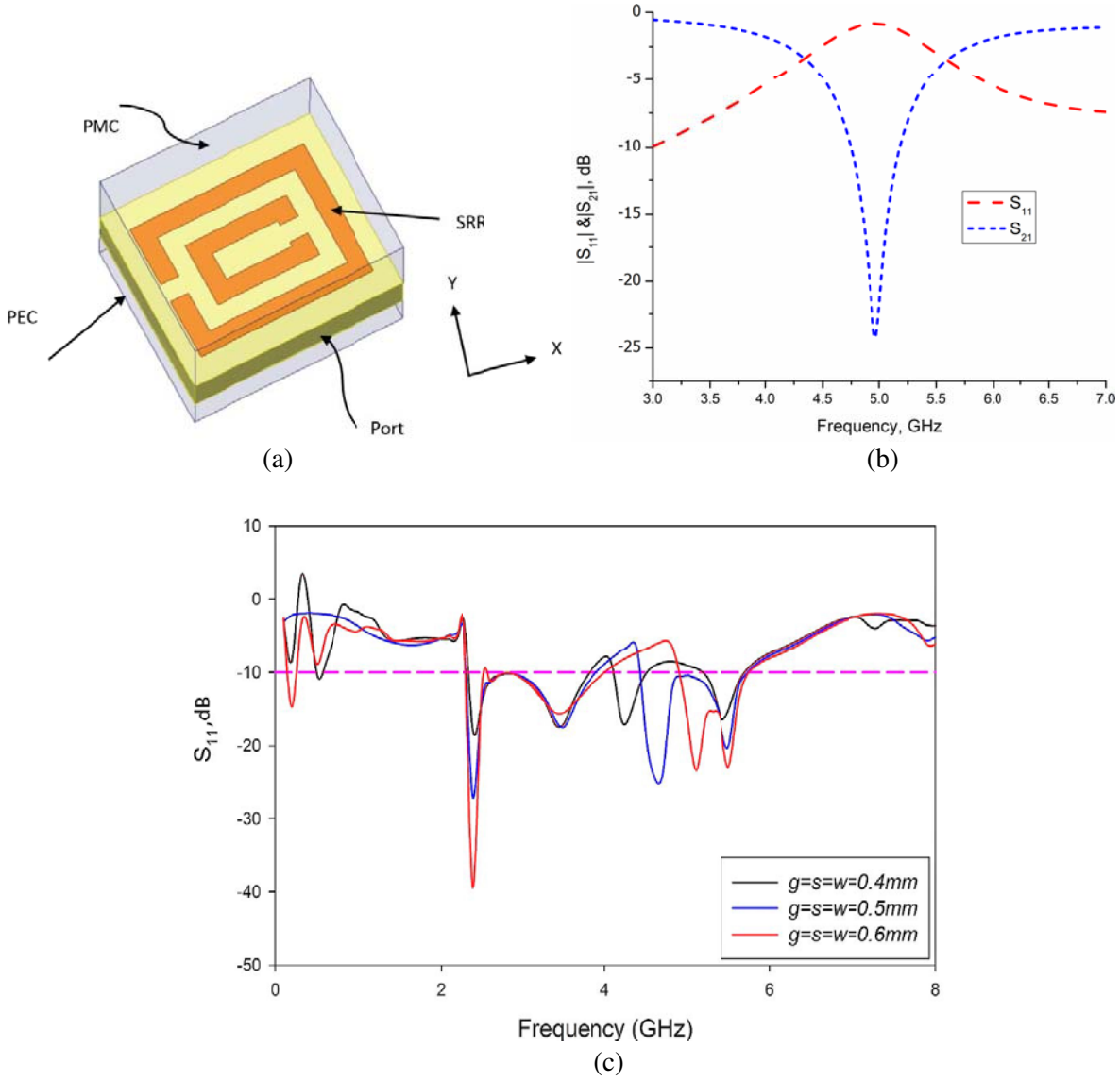

Figure 3. (a) Waveguide setup for the proposed antenna, (b) S-parameter extraction of the SRR and (c) S-parameter graph for different width and slot gap values of SRR.

SMA connectors, low cost FR-4 substrate, and manufacturing of the antenna prototype. The resonances after the addition of SRRs are achieved at 2.4 GHz, 3.5 GHz, and 5.3 GHz with IBW of 10%, 23.5%, and 17.2%, respectively. It can be used to cover ISM, WLAN, 4G LTE, and 5G applications. In spite of the compact area ($0.094\lambda_0^2$, where λ_0 is the highest operating wavelength) with the presence of common ground which exhibits high inter-element Isolation in all the working bands. The fabricated prototype of the proposed antenna and radiation pattern measurement setup is shown in Figs. 5(a)–5(c).

4. CURRENT DISTRIBUTION AND RADIATION CHARACTERISTICS

Current distribution characteristics describe the origin of particular resonances. From the current density figures obtained from the software simulation, we can notice that the 2.4 GHz band is formed by the combined effect of the four ILAs and slotted ground as seen in Fig. 6(a). Further, the 3.5 GHz band is due to the radiation from the ILAs, and the resonance at 5.1 GHz (Figs. 6(b)–(c)) is due to the SRRs that are placed close to the ILAs. SRRs are excited rationally symmetric to produce 5.1 GHz band

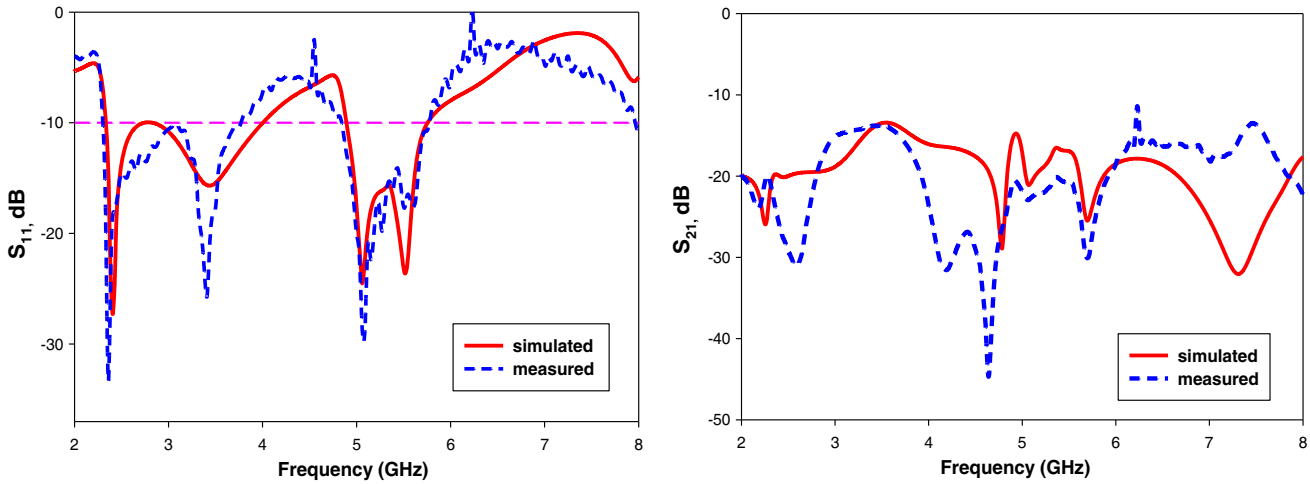

Figure 4. (a) Simulated and measured S_{11} values and (b) simulated and measured S_{21} values.

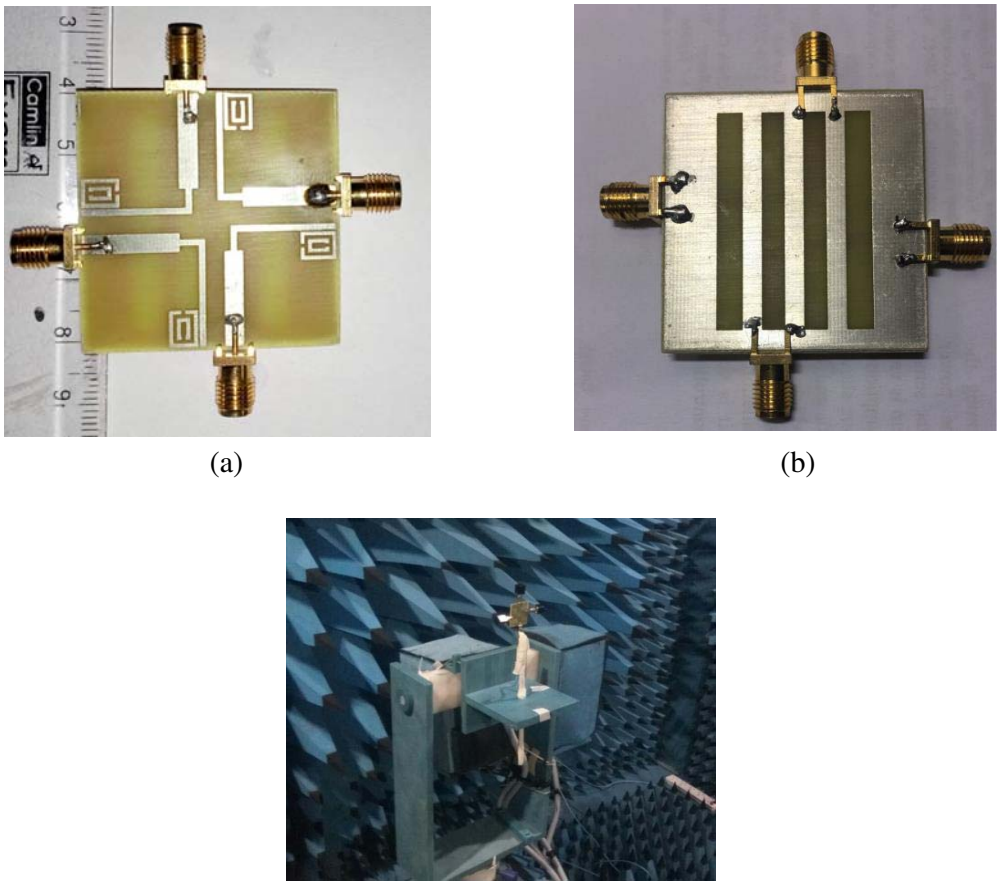

Figure 5. Fabricated prototype of the proposed antenna. (a) Top view, (b) bottom view and (c) pattern measurement setup in anechoic chamber.

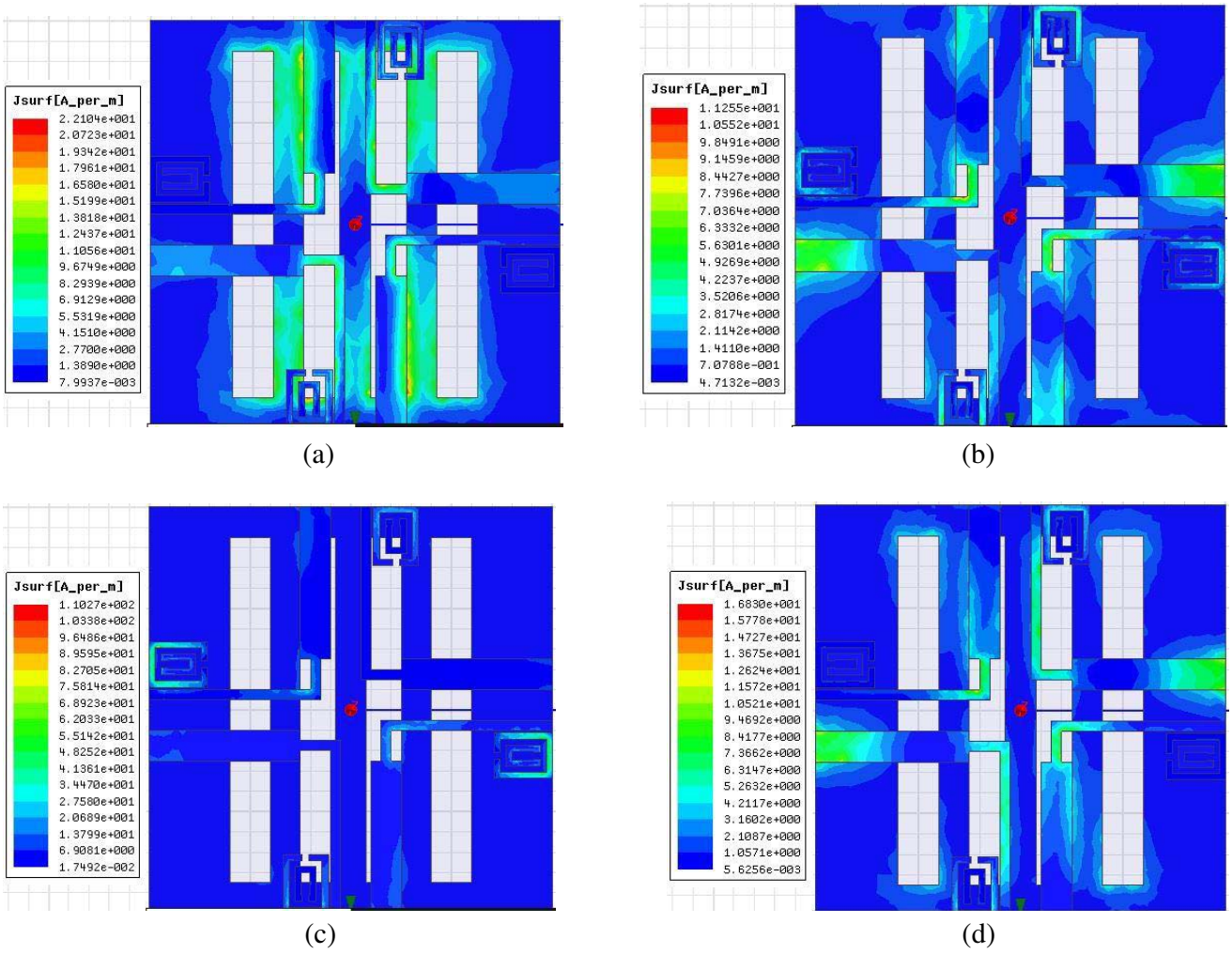

Figure 6. Surface current distributions (a) 2.4 GHz, (b) 3.5 GHz, (c) 5.1 GHz band and (d) 5.5 GHz.

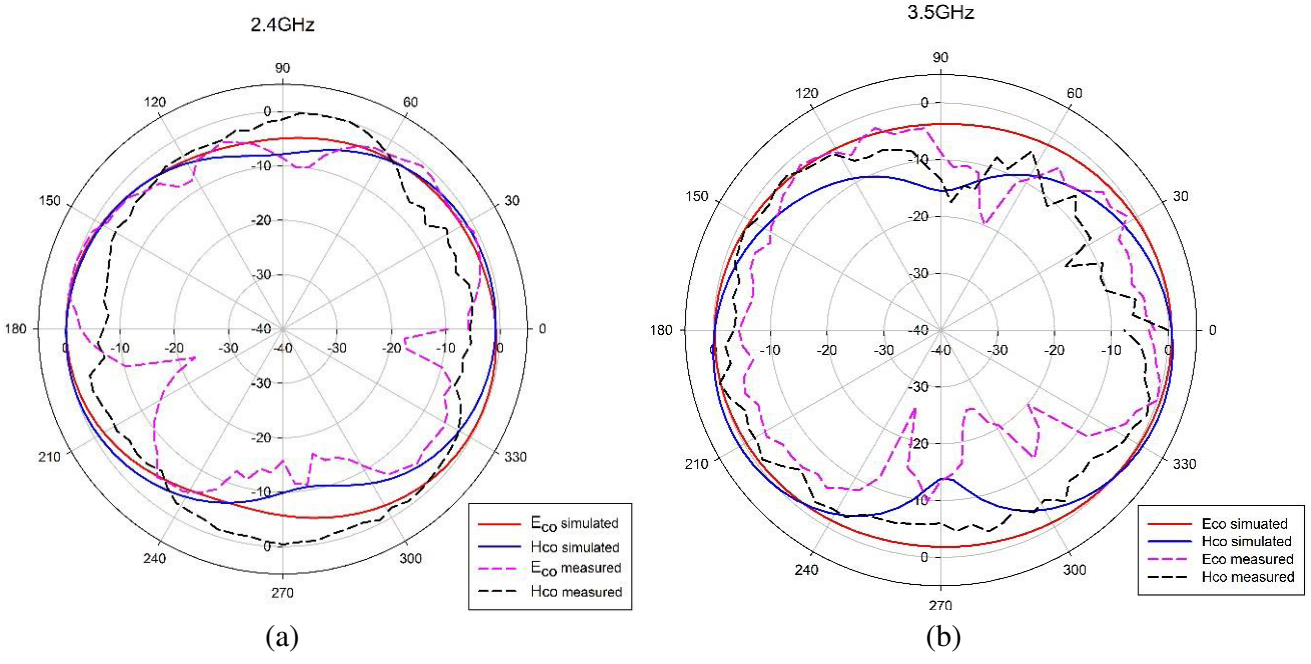

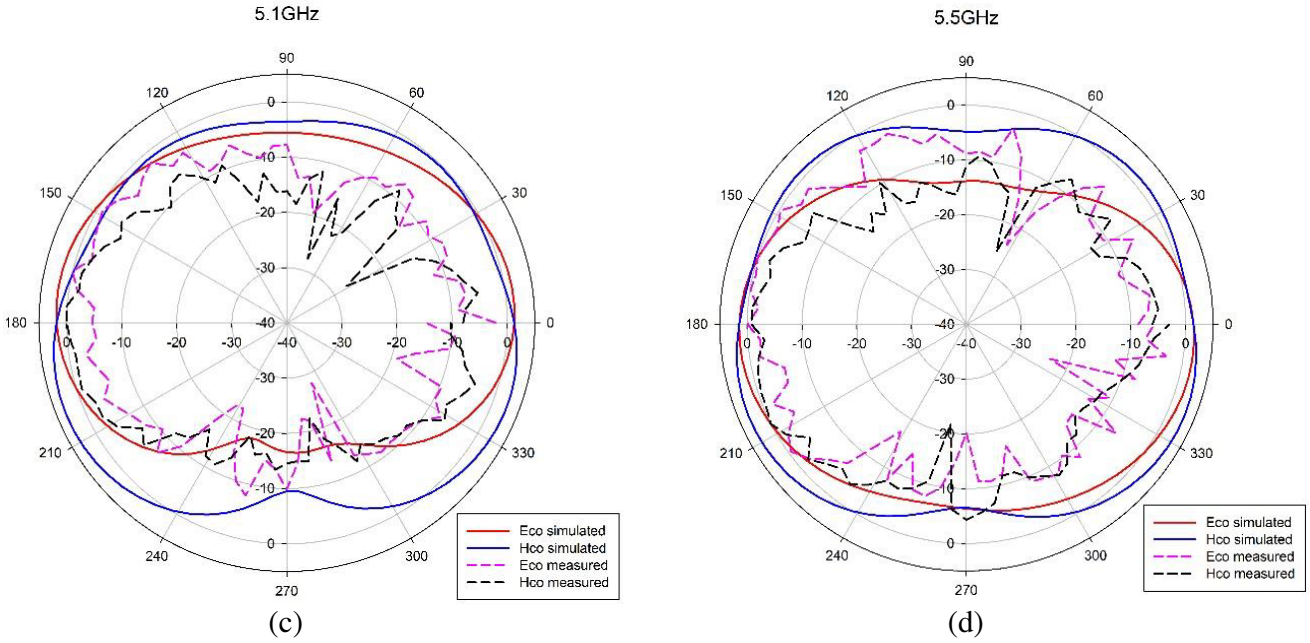

Figure 7. Simulated and measured radiation characteristics of the proposed antenna at (a) 2.4 GHz, (b) 3.5 GHz, (c) 5.1 GHz, (d) 5.5 GHz.

whereas 5.5 GHz band is the result of the combined excitation of SRR and ILA as shown in Fig. 6(d).

Figure 7 represents simulated and measured radiation patterns of the MIMO antenna for the operating frequencies. The E-plane and H-plane patterns represent the gain experienced in a particular direction. The radiation pattern shows omnidirectional characteristics in H-plane and eight shaped patterns in E-plane. The slight mismatch between simulated and measured radiation patterns is present at higher frequencies due to various reasons such as excitation of higher order modes, dielectric loss, soldering error of SMA connectors, and losses from connecting cables used in the measurement environment.

5. CONCLUSION

A compact MIMO antenna loaded with SRR for 2.4 GHz ISM/WLAN, 3.5 GHz WiMAX, and 5 GHz WLAN 4G/5G applications has been presented. In spite of very compact area ($0.094\lambda_0^2$, for highest operating wavelength) with the presence of common ground, the antenna exhibits high inter-element isolation (I) of ≥ -14 dB and good impedance matching in all the operating bands ($S_{11} \geq -10$ dB). The added advantage for the proposed antenna, compared to that of other existing designs in Table 1, is three operating bands which work only in frequencies that are more specific to the wireless applications and thus have high immunity for interference from unwanted signals. Overall, the proposed antenna is suitable for imminent multiband wireless terminal devices as it possesses significant impedance matching, radiation characteristics, and isolation as demanded in MIMO antenna systems.

REFERENCES

1. Panda, A. K., S. Sahu, and R. K. Mishra, "A compact dual-band 2×1 metamaterial inspired MIMO antenna system with high port isolation for LTE and WiMAX applications," *Int. J. RF Microw. Comput. Aided Eng.*, Vol. 27, 1–11, 2017.
2. Chouhan, S., D. K. Panda, M. Gupta, and S. Singhal, "Meander line MIMO antenna for 5.8 GHz WLAN application," *Int. J. RF Microw. Comput. Aided Eng.*, Vol. 28, No. 4, 1–8, 2017.
3. *Spectrum for 4G and 5G*, Qualcomm Technologies, Inc., San Diego, CA, USA, 2017.

4. Sharma, A., G. Das, and R. K. Gangwar, "Dual polarized triple band hybrid MIMO cylindrical dielectric resonator antenna for LTE2500/WLAN/WiMAX applications," *Int. J. RF Microw. Comput. Aided Eng.*, Vol. 26, No. 9, 763–772, 2016.
5. Lee, J.-G., D.-J. Kim, and J.-H. Lee, "Improvement of isolation andenvelop correlation coefficient using c-loaded $\lambda/4$ loop antenna on hollow ground," *Microw. Opt. Technol. Lett.*, Vol. 58, No. 9, 2189–2194, 2016.
6. Yu, X., L. Wang, H. G. Wang, X. Wu, and Y.-H. Shang, "A novel multiport matching method for maximum capacity of an indoor MIMO system," *Progress In Electromagnetics Research*, Vol. 130, 67–84, 2012.
7. Abdullah, M., Y. L. Ban, and K. Kang, "Compact 4-port MIMO antenna system for 5G mobile terminal," *Applied Computational Electromagnetics Society Symposium (ACES)*, 1–2, 2017.
8. Ahmed, F., Md. H. M. Chowdhury, and A. Md. A. Rahman, "A multiband MIMO antenna for future generation handset applications," *IEEE Conference on Electrical, Computer and Communication Engineering*, 91–94, 2017.
9. Singh, B. V., M. Agarwal, and M. K. Meshram, "F-shaped monopole based MIMO antenna for WLAN applications," *IEEE International Conference on Electrical, Computer and Electronics Engineering*, 576–579, 2016.
10. Hao, C., H. Zheng, J. Zhang, and X. Sun, "The deployment of stub structures for mutual coupling reduction in MIMO antenna applications," *Progress In Electromagnetics Research Letters*, Vol. 92, 39–45, 2020.
11. Nguyen, N. L., "Gain enhancement in MIMO antennas using defected ground structure," *Progress In Electromagnetics Research M*, Vol. 87, 127–136, 2019.
12. Sharma, K. and G. P. Pandey, "Two port compact MIMO antenna for ISM band applications," *Progress In Electromagnetics Research C*, Vol. 100, 173–185, 2020.
13. Ambika, A. and C. Tharini, "Semicircle CSRR with circular slot array structures for high level mutual coupling reduction in MIMO antenna," *Progress In Electromagnetics Research M*, Vol. 87, 23–32, 2019.
14. Moradi Kordalivand, A., T. A. Rahman, and M. Khalily, "Common elements wideband MIMO antenna system for WiFi/LTE access-point applications," *IEEE Antennas Wireless Propag. Lett.*, Vol. 13, No. 4, 1601–1604, 2014.
15. Wang, H., L. Liu, and Z. Zhang, "A wideband compact WLAN/ WiMAX MIMO antenna based on dipole with V-shaped ground branch," *IEEE Trans. Antennas Propag.*, Vol. 63, No. 5, 2290–2295, 2015.
16. Liao, K. C., W. S. Chen, and C. Y. D. Sim, "Massive MIMO 5G small cell antenna with high isolation," *Proc. Int. Workshop on Electromagnetics: Applications and Student Innovation Competition (iWEM)*, 1–4, 2017.
17. Sarkar, D. and K. V. Srivastava, "A compact four element MIMO/diversity antenna with enhanced bandwidth," *IEEE Antennas Wireless Propag. Lett.*, Vol. 16, 2469–2472, 2017.
18. Liu, P., D. Sun, P. Wang, and P. Gao, "Design of a dual-band MIMO antenna with high isolation for WLAN applications," *Progress In Electromagnetics Research Letters*, Vol. 74, 23–30, 2018.
19. Wu, W., R. Zhi, Y. Chen, H. Li, Y. Tan, and G. Liu, "A compact multiband MIMO antenna for IEEE 802.11 a/b/g/n applications," *Progress In Electromagnetics Research Letters*, Vol. 84, 59–65, 2019.
20. Dkiouak, A., A. Zakriti, M. El Ouahabi, A. Zugari, and M. Khalladi, "Design of a compact MIMO antenna for wireless applications," *Progress In Electromagnetics Research M*, Vol. 72, 115–124, 2018.
21. Nirmal, P. C., A. B. Nandgaonkar, S. L. Nalbalwar, and R. K. Gupta, "A compact dual band MIMO antenna with improved isolation for Wi-Max and WLAN applications," *Progress In Electromagnetics Research M*, Vol. 68, 69–77, 2018.
22. Sarkar, D., K. Saurav, and K. V. Srivastava, "A compact four element CSRR-loaded antenna for dual band pattern diversity MIMO applications," *Proc. 46th IEEE European Microwave Conf.*

(EuMC), 1315–1318, 2016.

23. Sarkar, D. and K. V. Srivastava, "Compact four-element SRR-loaded dual band MIMO antenna for WLAN/WiFi/4G-LTE and 5G applications," *IET Electron. Lett.*, Vol. 53, No. 25, 623–1624, 2017.
24. Anitha, R., P. V. Vinesh, K. C. Prakash, P. Mohanan, and K. Vasudevan, "A compact quad element slotted ground wideband antenna for MIMO applications," *IEEE Trans. Antennas Propag.*, Vol. 64, No. 10, 4550–4553, 2016.
25. Saurav, K., D. Sarkar, and K. V. Srivastava, "Multi-band circularly polarized cavity backed crossed dipole antenna," *IEEE Trans. Antennas Propag.*, Vol. 63, No. 10, 4286–4296, 2015.